



## THE DISTRIBUTION CHARACTERISTICS OF TURBULENT DISSIPATION RATE IN NOZZLE FLOWMETER

Feng Wang\*, Sen-Da Qi, Jiang-Bo Tong, Zi-Yan Hu, Yao-Qian Wang, Cheng-Xi Chai,  
Shi-Shi Jiang, Bo-Jie Xu

College of Mechanical Engineering, Quzhou University, Quzhou, 324000, China.

Article Received on 28/11/2020

Article Revised on 18/12/2020

Article Accepted on 08/01/2021

### \*Corresponding Author

Feng Wang

College of Mechanical  
Engineering, Quzhou  
University, Quzhou,  
324000, China.

### ABSTRACT

In this paper, the internal turbulent dissipation rate of nozzle flowmeter under different working conditions is studied, and its distribution characteristics are found. The physical model is used to model, and the motion law is obtained by using the knowledge of fluid mechanics and Navier Stokes equation. In this study, eight kinds of steady flow values

were used for the experiment, the experimental results show that the turbulent dissipation rate of the nozzle flowmeter is positively correlated with the flow rate. The results of this paper can be used for more accurate analysis of nozzle flowmeter, and can also be used to provide theoretical basis for the optimization of nozzle flowmeter equipment.

**KEYWORDS:** Nozzle flowmeter, numerical calculation, different flow rate, turbulence dissipation rate distribution.

### 1. INTRODUCTION

Nozzle steam flowmeter is widely used in the flow measurement of high temperature and high pressure fluid in electric power, chemical industry and other industries.<sup>[1]</sup> The research on the influence of working conditions on the distribution characteristics of turbulent dissipation rate in nozzle flowmeter can make the nozzle flowmeter more suitable for the equipment in life and various environments. Before that, Zhuang Guohua and others studied the inspection method of nozzle flowmeter used in main steam pipe of power plant boiler.<sup>[2-4]</sup> Zhao Xiangyuan studied the wide application of nozzle steam flowmeter in air separation,

which can well reflect the operation efficiency of steam turbine and compressor in practical application, and its accuracy and reliability play an important role in factory assessment.<sup>[5]</sup> At the same time, Wang Xin and Wang Xiaodong studied the application of fluid mechanics theory in flow measurement, and gave the classical application and derivation process of Bernoulli equation and continuity equation in flow.<sup>[6-8]</sup> Most of the above research focuses on the nozzle flowmeter itself, while this paper focuses on the external environment, that is, the influence of different working conditions on the nozzle flowmeter. The research results of this paper hope to help to use nozzle flowmeter more reasonably in different environments.

## 2. RESEARCH OBJECT AND METHOD

### 2.1 Physical model

The upstream surface of the nozzle flowmeter consists of a plane perpendicular to the axis, a cylindrical throat and possible grooves or inclined angles. As shown in Figure 1, it has a total length of 250 mm, a total width of 358 mm and a nominal diameter of 213 mm.

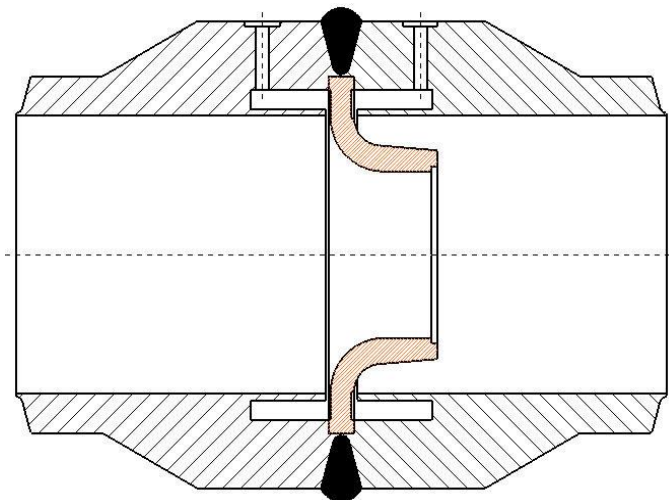


**Figure 1: Overall structure of nozzle flowmeter.**

### 2.2 Control equation

According to fluid mechanics, for incompressible viscous fluid in rectangular coordinate system, its motion law is controlled by Navier Stokes equations, The forms of the continuity equation and momentum equation are as follows

$$\frac{\partial \mu}{\partial x} + \frac{\partial v}{\partial y} = 0 \quad (1)$$

$$\rho u \frac{\partial u}{\partial x} + \rho v \frac{\partial u}{\partial y} = -\frac{\partial p}{\partial x} + \frac{\partial}{\partial y} \left( \eta \frac{\partial u}{\partial y} \right) \quad (2)$$

### 2.3 Computing method

In standard conditions, set the fluid properties, The fluid medium is water, The density is  $\rho = 1 \text{ kg/m}^3$ , dynamic viscosity is  $\eta = 0.001 \text{ Pa} \cdot \text{s}$ . In order to get accurate calculation, The simple scheme is used to solve the pressure term and the velocity term. For the sake of the size effect of standard nozzle forging on the calculation results, then  $\mu = U, v = 0$ . Set the standard nozzle core to no penetration, no slip requirement. Namely  $\mu = 0, v = 0$ .

### 2.4 Calculation scheme

The identification of key surface of nozzle flowmeter is of great significance to the study of internal flow characteristics. The identification of the four faces is shown in Figure 2, where Face 1 represents the upstream face of the nozzle and Face 2 represents the downstream outlet surface of the nozzle, Face 3 represents the outlet surface of the nozzle flowmeter, and Face 4 represents the horizontal plane passing through the central axis of the nozzle flowmeter. The surface line identification of nozzle flowmeter is shown in Figure 3, where Line 11 is the center line of flowmeter.

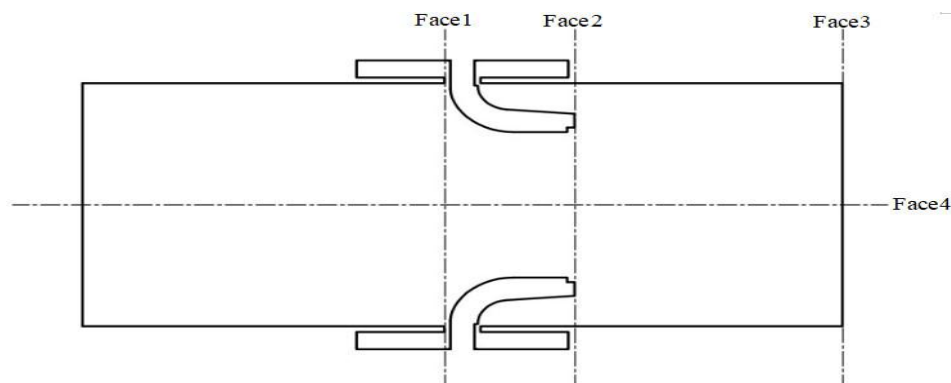


**Figure 2: Identification drawing of nozzle flowmeter surface.**

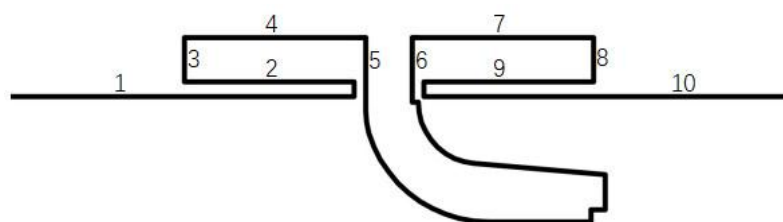


**Figure 3: Surface line identification of nozzle flowmeter.**

In order to study the flow rate distribution of the flow meter under different turbulent flow rate. In this study, 8 kinds of stable flow values will be taken, namely 5, 25, 50, 125, 250, 500, 750, and  $1000 \text{ m}^3/\text{h}$ . The calculation scheme is shown in Table 1.

**Table 1: Calculation scheme.**

Calculation scheme(case)	No.1	No.2	No.3	No.4	No.5	No.6	No.7	No.8
Working condition flow( m <sup>3</sup> /h)	5	25	50	125	250	500	750	1000

For the study of four identification surfaces, choosing the steady flow value as 5, 25, 125, and 750 m<sup>3</sup>/h. Among them, 5 m<sup>3</sup>/h refers to ultra-small flow condition, 25 m<sup>3</sup>/h refers to small flow condition, 125 m<sup>3</sup>/h medium and small flow condition, and 750 m<sup>3</sup>/h large flow condition.

### 3. RESULT ANALYSIS

(a), (b), (c) and (d) in the following cloud images represent Face1, Face2, Face3 and Face4, respectively. While (a), (b), (c), (d), (e), (f), (g), (h), (i), (j) and (k) denote Line1, Line2, Line3, Line4, Line5, Line6, Line7, Line8, Line9, Line10 and Line11, respectively.

#### 3.1 Turbulent dissipation rate distribution

The turbulent dissipation rate distribution of the nozzle flowmeter at ultra-small flow rate (5 m<sup>3</sup>/h) is shown in Figure 4. When the inlet flow rate is 5m<sup>3</sup>/h, the maximum turbulent dissipation rate of Face 1 appears at a point in the second layer of the surface, and its value is 0.018. The minimum turbulent dissipation rate appears in the outer ring of the surface, and its value is 0.002. The turbulence dissipation rate at the second layer changes obviously, and the turbulence dissipation rate of different values is distributed on this surface. The maximum turbulent dissipation rate of Face 2 is 0.0014, and the minimum turbulent dissipation rate is 0.002 at the center of the surface. The results show that the turbulent dissipation rate changes obviously in the outer ring. The maximum turbulent dissipation rate of Face 3 appears at the outermost layer of the surface, and its value is 0.0014. The minimum turbulent dissipation rate appears in the inner circle of the surface, and its value is 0.002. The turbulent dissipation rate under obvious change is concentrated in the outer ring. The maximum turbulent dissipation rate of Face 4 is 0.1 at the nozzle turning point, and the minimum turbulent dissipation rate is 0.01 except for the nozzle turning point. It can be seen from the figure that the overall trend of the key components is not affected by the turbulence dissipation rate, and the places affected by the turbulence dissipation rate are only in some key positions.

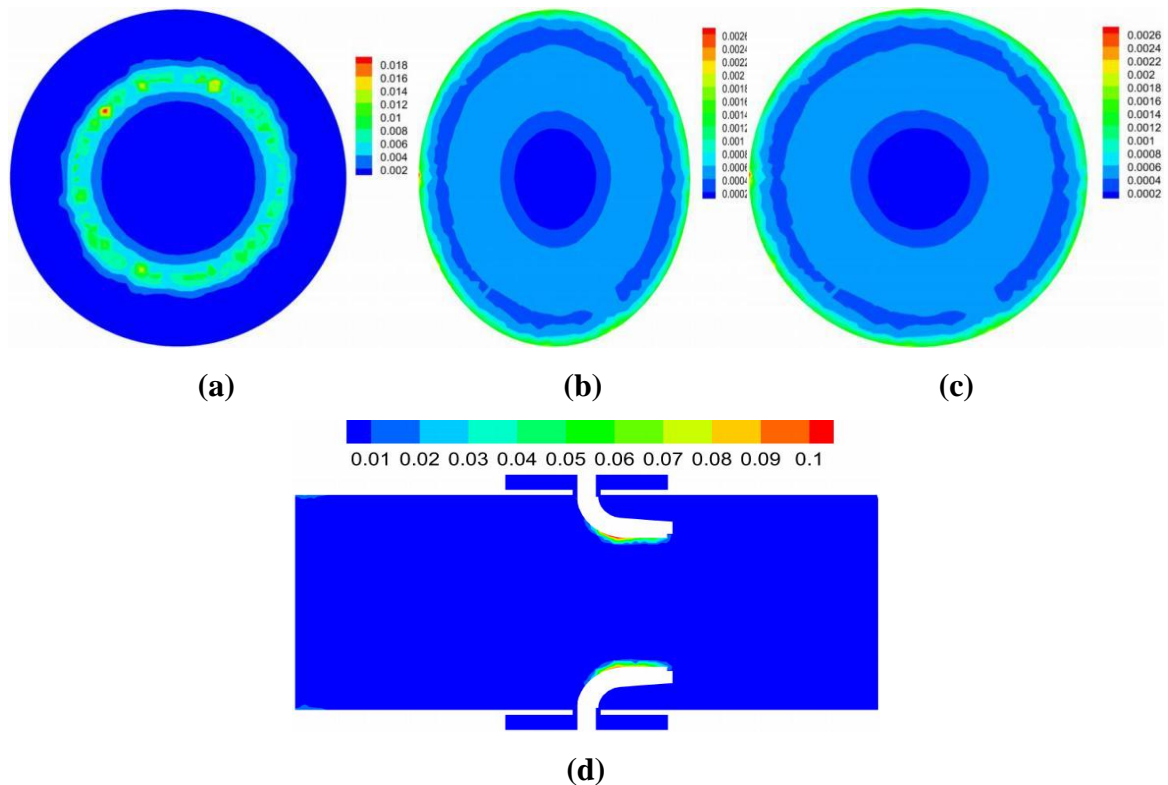


**Figure 4: Distribution of turbulent dissipation rate at very small flow rate ( $5\text{m}^3/\text{h}$ ).**

The turbulent dissipation rate distribution of nozzle flowmeter at small flow rate ( $25\text{m}^3/\text{h}$ ) is shown in Figure 5. When the inlet flow rate is  $25\text{m}^3/\text{h}$ , the maximum turbulent dissipation rate of Face 1 is evenly distributed in the middle layer, and its value is 0.025. The minimum turbulent dissipation rate appears in the outermost circle and inner circle of the surface, and its value is 0.005. It can be seen from the figure that there are different values of turbulent dissipation rate in the middle layer. The maximum turbulent dissipation rate of Face 2 appears in the small area of the middle circle of the downstream outlet of the nozzle, and its value is 0.8. The minimum turbulent dissipation rate appears in the outermost circle and inner ring of the surface, and its value is 0.1. It can be seen from the figure that there are different values of turbulent dissipation rate in the middle circle layer. The maximum turbulent dissipation rate of Face 3 appears at the outermost ring of the nozzle flowmeter, and its value is 0.1. The minimum turbulent dissipation rate appears in the inner ring of the nozzle flowmeter, and its value is 0.02. There is no obvious change rule in this figure, but it can be seen that the main turbulence dissipation rate is concentrated in the outermost ring. The maximum turbulent dissipation rate of Face 4 is 3.4 at the nozzle turning point, and the minimum turbulent dissipation rate is 0.2 outside the nozzle turning point.

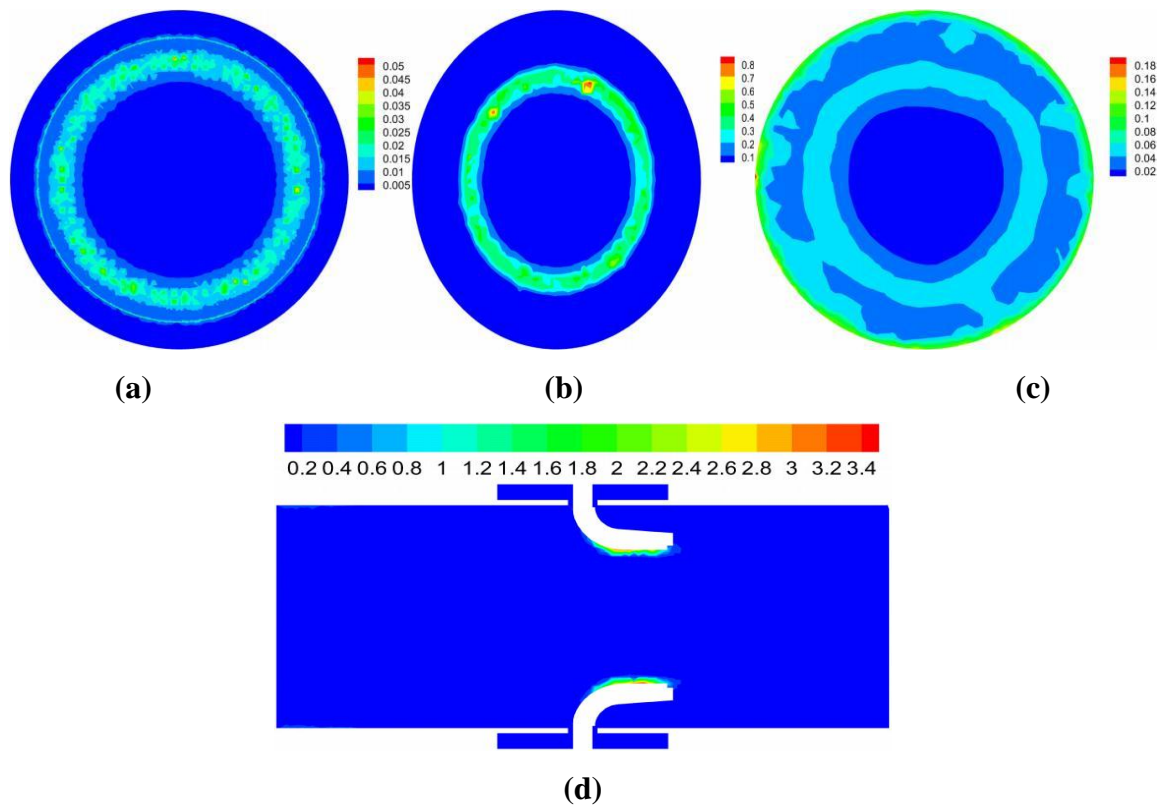


**Figure 5: Distribution of turbulent dissipation rate at small flow rate ( $25\text{m}^3/\text{h}$ ).**

The turbulent dissipation rate distribution of nozzle flowmeter at medium and small flow rate ( $125\text{m}^3/\text{h}$ ) is shown in Figure 6. When the inlet flow rate is  $125\text{m}^3/\text{h}$ , the maximum turbulent dissipation rate of Face 1 appears in the outer circle, which is 1.6. The minimum turbulent dissipation rate mainly occurs in the outermost layer and the innermost ring layer, with a value of 0.2, and the main turbulence dissipation rate changes in the middle layer. The maximum turbulent dissipation rate of Face 2 rarely appears in the central layer of this surface, and its value is 60. The minimum turbulent dissipation rate appears in the outermost and innermost rings of the surface, and its value is 5. It can be seen from the figure that there are different values of turbulent dissipation rate in the middle layer; The maximum turbulent dissipation rate of Face 3 appears in a small part of the outer ring, which is 45, and the minimum turbulence dissipation rate is 5 in the inner ring of the face. The maximum turbulent dissipation rate of Face 4 appears at the point below the inflection point of nozzle arc, and its value is 70. The minimum turbulent dissipation rate appears at the entrance, step and outlet of nozzle flowmeter, and its value is 5.



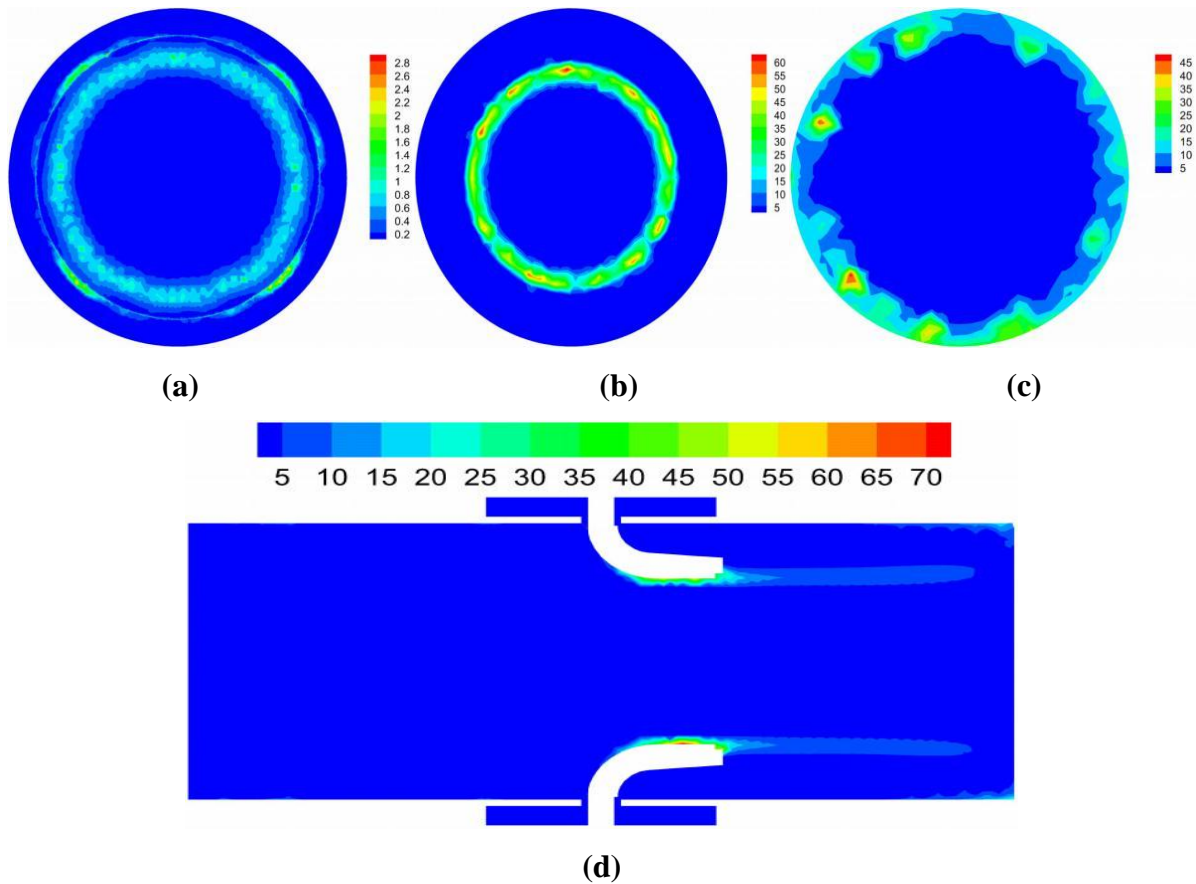


**Figure 6: Distribution of turbulent dissipation rate at small and medium flow rates ( $125\text{m}^3/\text{h}$ ).**

The turbulent dissipation rate distribution of nozzle flowmeter at large flow rate ( $750\text{m}^3/\text{h}$ ) is shown in Figure 7. When the inlet flow rate is  $750\text{m}^3/\text{h}$ , the maximum turbulent dissipation rate of Face 1 occupies a large area on the upstream surface of the nozzle, and its value is 50, and the minimum turbulent dissipation rate is scattered on this surface, and its value is 200. From this figure, it can be seen that there is no turbulence dissipation rate with particularly large value for the key parts; The maximum turbulent dissipation rate of Face 2 is 12000 in the middle layer, and the minimum turbulence dissipation rate is 1000 in the outer and inner rings of the surface, and the main turbulence dissipation rate changes in the middle layer; The maximum turbulent dissipation rate of Face 3 appears in the small area near the outermost layer, and its value is 10000. The minimum turbulent dissipation rate appears in the inner circle of the surface, with the value of 1000. The area of the maximum turbulent dissipation rate only occupies the local area of the whole figure; The maximum turbulent dissipation rate of Face 4 is 8000 at the end of nozzle, and the minimum turbulence dissipation rate is 500 at the entrance, steps and some outlets of the nozzle flowmeter.

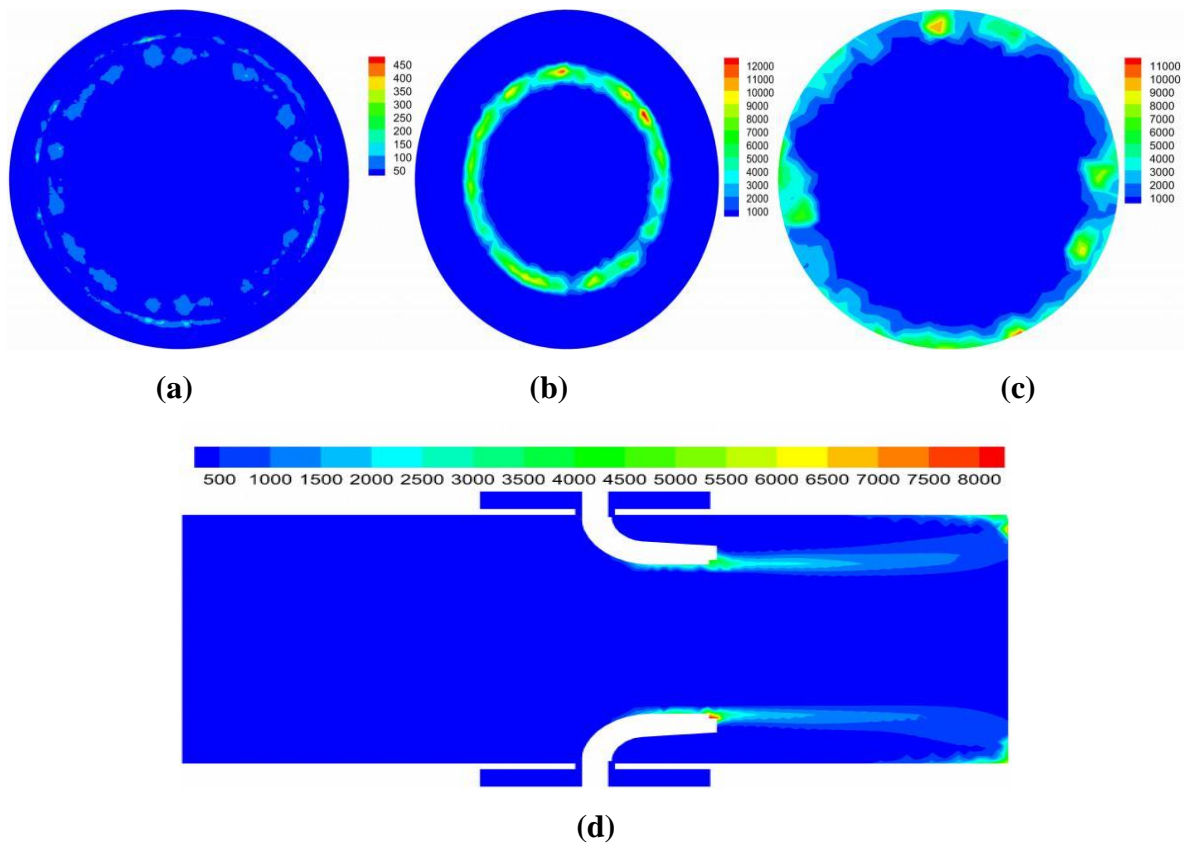


**Figure 7: Distribution of turbulent dissipation rate at large flow rate (750m<sup>3</sup>/h).**

### 3.2 Turbulent dissipation rate at boundary

The turbulent dissipation rate distribution of the nozzle flowmeter at the boundary is shown in Figure 8. Therefore, the turbulent dissipation rate of each fluid surface will still be different.

In Figure 8 (a), the turbulent dissipation rate of Line1 is not obvious at small flow rate, but is obvious at large flow rate. When the flow rate is 250m<sup>3</sup>/h, the turbulent dissipation rate of Line1 tends to be stable at 20 m<sup>2</sup>/s<sup>3</sup>. When  $l$  is 0.75, the turbulent dissipation rate reaches the maximum value, which is 35m<sup>2</sup>/s<sup>3</sup>, and then decreases to 0 m<sup>2</sup>/s<sup>3</sup>. When the flow rate is 500 m<sup>3</sup>/h, the turbulent dissipation rate of Line1 initially fluctuates around 60 m<sup>2</sup>/s<sup>3</sup>. When  $l$  is 0.78, the turbulent dissipation rate reaches the maximum value, which is 230m<sup>2</sup>/s<sup>3</sup>, and then decreases to nearly 0 m<sup>2</sup>/s<sup>3</sup>. When the flow rate is 750m<sup>3</sup>/h, the turbulent dissipation rate of Line1 initially fluctuates around 110 m<sup>2</sup>/s<sup>3</sup>. When  $l$  is 0.78, the turbulent dissipation rate reaches the maximum value, which is 520m<sup>2</sup>/s<sup>3</sup>, and then decreases to 0 m<sup>2</sup>/s<sup>3</sup>. When the flow rate is 1000 m<sup>3</sup>/h, the turbulent dissipation rate of Line1 fluctuates from 220 m<sup>2</sup>/s<sup>3</sup> at the beginning. When  $l$  is 0.78, the turbulent dissipation rate reaches the maximum value, which is 860 m<sup>2</sup>/s<sup>3</sup>, and then decreases to 140 m<sup>2</sup>/s<sup>3</sup>.



In Figure 8 (b), the turbulent dissipation rate of line2 is not obvious at the beginning, and fluctuates around  $0 \text{ m}^2/\text{s}^3$ . When  $l$  is 0.8, the turbulent dissipation rate of line2 increases gradually at large flow rate. When the flow rate is  $250 \text{ m}^3/\text{h}$  and  $1000 \text{ m}^3/\text{h}$ , the turbulence dissipation rate has a coincidence part, but the maximum turbulent dissipation rate is  $0.8 \text{ m}^2/\text{s}^3$ . When the flow rate is  $500 \text{ m}^3/\text{h}$  and  $750 \text{ m}^3/\text{h}$ , and when  $l$  is 0.94, the maximum turbulent dissipation rate reaches  $3.6 \text{ m}^2/\text{s}^3$  and  $2.4 \text{ m}^2/\text{s}^3$ , respectively.

In Figure 8 (c), the turbulent dissipation rate of Line3 is not obvious when the flow rate is lower than  $125 \text{ m}^3/\text{h}$ , and the turbulent dissipation rate of Line3 remains  $0 \text{ m}^2/\text{s}^3$ . When the flow rate is  $250 \text{ m}^3/\text{h}$ , the turbulent dissipation rate is about  $0.001 \text{ m}^2/\text{s}^3$ . When the flow rate is  $1000 \text{ m}^3/\text{h}$ , the turbulent dissipation first increases to the highest point and then decreases gradually. When  $l$  is 0.5, the turbulent dissipation rate reaches the maximum value of  $0.025 \text{ m}^2/\text{s}^3$ . When the flow rate is  $500 \text{ m}^3/\text{h}$  and  $750 \text{ m}^3/\text{h}$ , the turbulence dissipation rate is partially overlapped. One is that when  $l$  is less than 0.3, the other is when  $l$  is 0.58, the overall trend of the turbulence dissipation rate is firstly increased and then decreased.

In Figure 8 (d), the turbulence dissipation rate of line4 fluctuates little under small flow rate, and when the flow rate is lower than  $125 \text{ m}^3/\text{h}$ , the turbulent dissipation rate is  $0 \text{ m}^2/\text{s}^3$ . When the flow rate is  $250 \text{ m}^3/\text{h}$ , the turbulent dissipation first increases and then decreases gradually. When  $l$  is 0.75, the maximum turbulent dissipation rate is 0.02. When the discharge is  $500 \text{ m}^3/\text{h}$ ,  $750 \text{ m}^3/\text{h}$  and  $1000 \text{ m}^3/\text{h}$ , the overall trend is that the oscillation fluctuates to the maximum value and then gradually decreases. When  $l$  is greater than 0.3 and less than 0.6, there is a coincidence between  $750 \text{ m}^3/\text{h}$  and  $1000 \text{ m}^3/\text{h}$ . When  $l$  is 0.78, the maximum turbulent dissipation rate exists at the flow rate of  $500 \text{ m}^3/\text{h}$  and  $1000 \text{ m}^3/\text{h}$ , which are  $0.06 \text{ m}^2/\text{s}^3$  and  $0.11 \text{ m}^2/\text{s}^3$ , respectively. When  $l$  is 0.85, there is a maximum turbulent dissipation rate of  $750 \text{ m}^3/\text{h}$ , which is  $0.15 \text{ m}^2/\text{s}^3$ .

In Figure 8 (e), when  $l$  is less than 0.5, the turbulent dissipation rate of line5 is  $0 \text{ m}^2/\text{s}^3$  at various flow rates. When  $l$  is greater than 0.5, the turbulent dissipation rate of line5 is still  $0 \text{ m}^2/\text{s}^3$  at low flow rate. When the flow rate is  $250 \text{ m}^3/\text{h}$ , the turbulence dissipation rate fluctuation is very small and not obvious. When the flow rate is  $500 \text{ m}^3/\text{h}$  and  $750 \text{ m}^3/\text{h}$ , the turbulent dissipation rate of line5 is more obvious, showing an upward trend. When the flow rate is  $500 \text{ m}^3/\text{h}$ , the maximum turbulent dissipation rate of line5 is close to  $50 \text{ m}^2/\text{s}^3$ , when the flow rate is  $750 \text{ m}^3/\text{h}$ , the maximum value of turbulence dissipation rate on line 5 is close

to  $300 \text{ m}^2/\text{s}^3$ , and when the flow rate is  $1000 \text{ m}^3/\text{h}$ , the turbulence dissipation rate of line5 is  $0 \text{ m}^2/\text{s}^3$ .

In Figure 8(f), the turbulent dissipation rate of line6 does not change significantly at small flow rate, and the turbulence dissipation rate of line6 is  $0 \text{ m}^2/\text{s}^3$ . When the flow rate increases gradually, the turbulent dissipation rate first increases and then decreases. When the flow rate is  $250 \text{ m}^3/\text{h}$  and  $l$  is 0.8, the maximum turbulent dissipation rate is  $10 \text{ m}^2/\text{s}^3$ ; when the flow rate is  $500 \text{ m}^3/\text{h}$  and  $l$  is 0.66, the maximum turbulence dissipation rate is  $10 \text{ m}^2/\text{s}^3$ ; when the flow rate is  $750 \text{ m}^3/\text{h}$  and  $l$  is 0.8, the maximum turbulence dissipation rate is  $120 \text{ m}^2/\text{s}^3$ ; when the flow rate is  $1000 \text{ m}^3/\text{h}$  and  $l$  is 0.68, the maximum turbulence dissipation rate is  $430 \text{ m}^2/\text{s}^3$ .

In Figure 8 (g), the turbulent dissipation rate of line7 is  $0 \text{ m}^2/\text{s}^3$  when  $l$  is greater than 0.7. When  $l$  is less than 0.7, the turbulence dissipation rate of line7 is close to  $0 \text{ m}^2/\text{s}^3$ . When the flow rate is  $500 \text{ m}^3/\text{h}$ ,  $750 \text{ m}^3/\text{h}$  and  $1000 \text{ m}^3/\text{h}$ , the turbulence dissipation rate increases first and then decreases. When the flow rate is  $1000 \text{ m}^3/\text{h}$ , the turbulence dissipation rate fluctuates most. When the flow rate is  $500 \text{ m}^3/\text{h}$  and  $l$  is 0.16, the maximum turbulent dissipation rate is  $10 \text{ m}^2/\text{s}^3$ ; when the flow rate is  $750 \text{ m}^3/\text{h}$  and  $l$  is 0.12, the maximum turbulence dissipation rate is  $22 \text{ m}^2/\text{s}^3$ ; when the flow rate is  $1000 \text{ m}^3/\text{h}$  and  $l$  is 0.12, the maximum turbulent dissipation rate is  $116 \text{ m}^2/\text{s}^3$ .

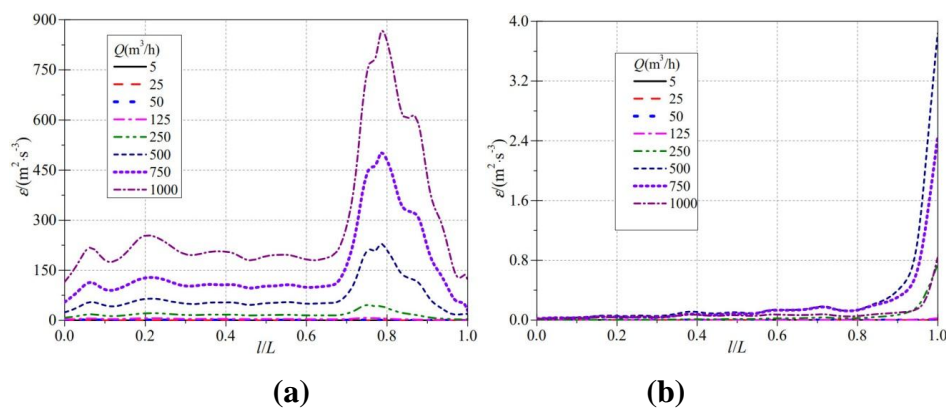
In Figure 8(h), the turbulent dissipation rate of Line8 does not change significantly at small flow rate, both of which are  $0 \text{ m}^2/\text{s}^3$ . When  $l$  is less than 0.3, the turbulent dissipation rate of Line8 at a flow rate of  $1000 \text{ m}^3/\text{h}$  is greater than that of a flow rate of  $750 \text{ m}^3/\text{h}$ , and there is an intersection point when  $l$  is 0.3, which is  $0.84 \text{ m}^2/\text{s}^3$ . When  $l$  is greater than 0.3 and less than 0.75, the turbulent dissipation rate of Line8 at a flow rate of  $1000 \text{ m}^3/\text{h}$  is less than that of a flow rate of  $750 \text{ m}^3/\text{h}$ . When  $l$  is greater than 0.75 and less than 1, the turbulent dissipation rate of Line8 at a flow rate of  $1000 \text{ m}^3/\text{h}$  is greater than that of a flow rate of  $750 \text{ m}^3/\text{h}$ , and there is an intersection point when  $l$  is 0.75, and its value is  $0.78 \text{ m}^2/\text{s}^3$ .

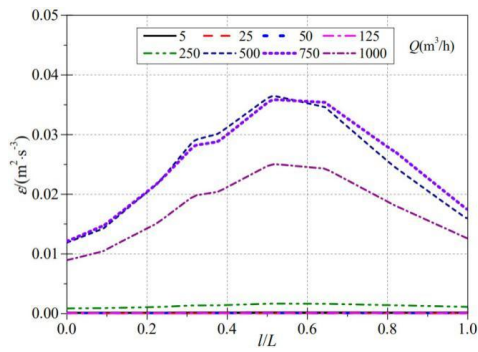
In Figure 8 (i), the turbulent dissipation rate of line9 is  $0 \text{ m}^2/\text{s}^3$  when  $l$  is greater than 0.6. When  $l$  is less than 0.6 and flow rate is less than  $250 \text{ m}^3/\text{h}$ , the turbulent dissipation rate of line9 almost keeps at  $0 \text{ m}^2/\text{s}^3$ . When the flow rate is  $500 \text{ m}^3/\text{h}$  and  $750 \text{ m}^3/\text{h}$ , the turbulence dissipation rate first decreases and then increases to  $0 \text{ m}^2/\text{s}^3$ . The flow rates of  $500 \text{ m}^3/\text{h}$  and  $750 \text{ m}^3/\text{h}$  coincide at  $L = 0.05$ , and the turbulent dissipation rate is  $0 \text{ m}^2/\text{s}^3$ . When the flow rate is  $1000 \text{ m}^3/\text{h}$ , the fluctuation of line9 is large, and the trend first decreases to the

minimum and then reaches the maximum value. Finally, with the increase of  $L$ , the turbulent dissipation rate tends to  $0 \text{ m}^2/\text{s}^3$ , the lowest value of the peak value is  $20 \text{ m}^2/\text{s}^3$ , and the maximum value is  $90 \text{ m}^2/\text{s}^3$ .

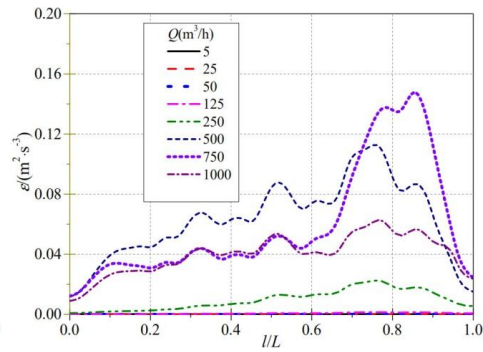
In Figure 8 (I), the turbulent dissipation rate of line9 is  $0 \text{ m}^2/\text{s}^3$  when  $l$  is greater than 0.6. When  $l$  is less than 0.6 and flow rate is less than  $250 \text{ m}^3/\text{h}$ , the turbulent dissipation rate of line9 almost keeps at  $0 \text{ m}^2/\text{s}^3$ . When the flow rate is  $500 \text{ m}^3/\text{h}$  and  $750 \text{ m}^3/\text{h}$ , the turbulence dissipation rate first decreases and then increases to  $0 \text{ m}^2/\text{s}^3$ . The flow rates of  $500 \text{ m}^3/\text{h}$  and  $750 \text{ m}^3/\text{h}$  coincide at  $L = 0.05$ , and the turbulent dissipation rate is  $0 \text{ m}^2/\text{s}^3$ . When the flow rate is  $1000 \text{ m}^3/\text{h}$ , the fluctuation of line9 is large, and the trend first decreases to the minimum and then reaches the maximum value. Finally, with the increase of  $L$ , the turbulent dissipation rate tends to  $0 \text{ m}^2/\text{s}^3$ , the lowest value of the peak value is  $20 \text{ m}^2/\text{s}^3$ , and the maximum value is  $90 \text{ m}^2/\text{s}^3$ .

In Figure 8 (k), line11 has almost no turbulent dissipation rate when  $l$  is less than 0.4, The turbulent dissipation rate is  $0 \text{ m}^2/\text{s}^3$ . When  $l$  is greater than 0.4, the turbulent dissipation rate increases gradually. With the increase of flow rate, the turbulence dissipation rate of line11 increases with the increase of  $L$ . When the flow rate is  $500 \text{ m}^3/\text{h}$ , the turbulent dissipation rate of line11 changes slightly. With the increase of  $L$ , the turbulence dissipation rate increases, and the maximum value is  $22 \text{ m}^2/\text{s}^3$ . When the flow rate is  $750 \text{ m}^3/\text{h}$ , the turbulent dissipation rate of line11 changes slightly. With the increase of  $L$ , the turbulence dissipation rate increases, and its maximum value is  $82 \text{ m}^2/\text{s}^3$ . When the flow rate is  $1000 \text{ m}^3/\text{h}$ , the turbulent dissipation rate of line11 changes greatly. With the increase of  $L$ , the turbulence dissipation rate increases, and the maximum value is  $202 \text{ m}^2/\text{s}^3$ .

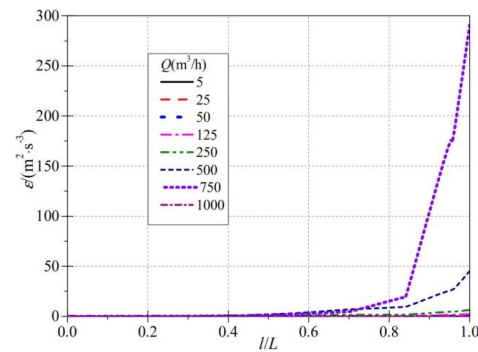




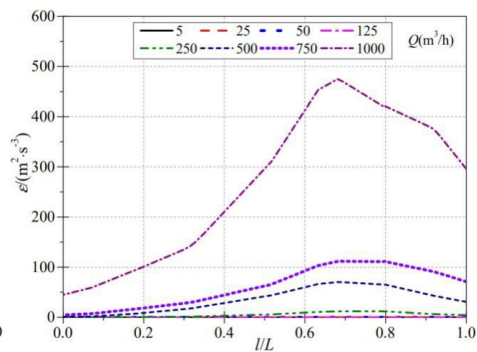
(c)



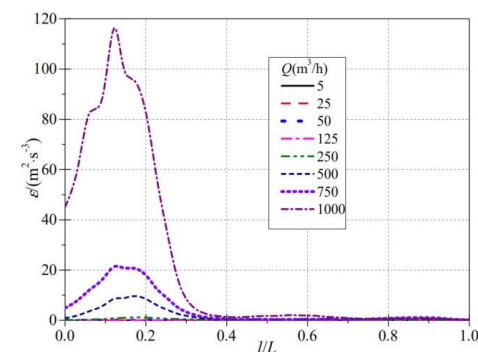
(d)



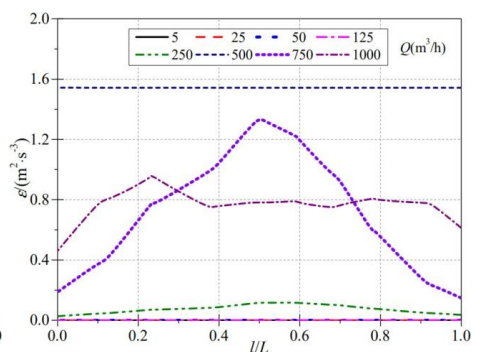
(e)



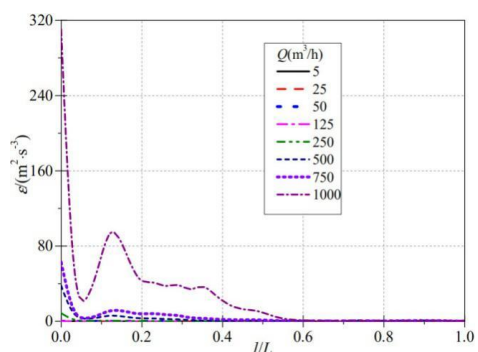
(f)



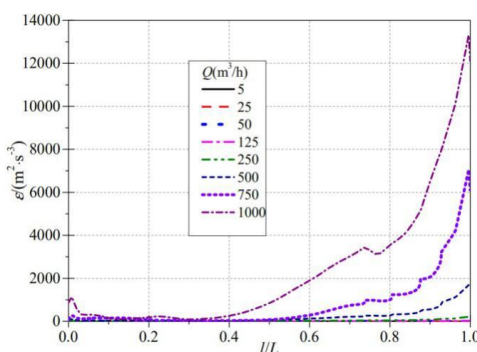
(g)



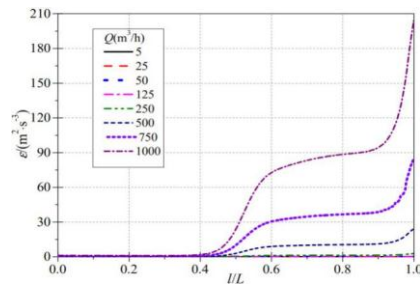
(h)



(i)



(j)



(k)

**Figure 8: Distribution of turbulent dissipation rate on the boundary.**

#### 4. CONCLUSION

In this paper, eight different flow values are tested in the same nozzle flowmeter :

1. The turbulent dissipation rate of the nozzle flowmeter is positively correlated with the flow rate.
2. The distribution of turbulent dissipation rate varies with the flow rate in the nozzle flowmeter.
3. For the nozzle flowmeter at the boundary, the turbulent dissipation rate on different fluid surfaces is different, and the consumption rate corresponding to different flow values is different, but the overall trend is similar.
4. When the boundary length of the nozzle flowmeter is different, the dissipation rate varies with the corresponding turbulence dissipation rate, but the trend is similar.

#### ACKNOWLEDGEMENTS

The work was supported by the national college students' science and technology innovation project (No. 202011488018).

#### REFERENCES

1. Luo Zhaoqiang, ya yunqi, Dai Enxian, et al. Research on the detection method of ISA 1932 nozzle steam flowmeter [J]. China Special Equipment Safety, 2019; 35(08): 19-24.
2. Zhao Chunyang. Application of differential pressure flowmeter in energy measurement [J]. Yizhong Technology, 2008; (04): 101-102.
3. Zhou Zhijian, Geng Xiuming. Application and discussion of new flow sensor [J]. Nonferrous Equipment, 2001; (06): 8-9-28.
4. Zhuang Guohua, Zhang Dechao, sun Lei. Discussion on inspection method of nozzle flowmeter in main steam pipe of power plant boiler [J]. Safety Technology of Special Equipment, 2020; (03): 6-9-62.

5. Zhao Xiangyuan. Application and analysis of nozzle flowmeter in air separation plant [J]. Internal Combustion Engine and Accessories, 2018; (07): 70-72.
6. Wang Xin, Wang Xiaodong, Zhang Xiaodong. Application of fluid mechanics theory in flow measurement [J]. Electronic World, 2013; (24): 190-191.
7. Zhong Wei. Numerical simulation and experimental study on flow field of throttling device for flow measurement [D]. Nanjing. Nanjing University of Aeronautics and Astronautics, 2007.
8. Sun Huaiqing. Lecture on "flow measurement method and instrument selection" - Lecture 25: field error estimation of flow measurement (1) [J]. Automatic Instrument, 1999; (03): 3-5.